© 2022. Published by The Company of Biologists Ltd | Journal of Experimental Biology (2022) 225, jeb243680. doi:10.1242/jeb.243680

RESEARCH ARTICLE

Interindividual variation in maximum aerobic metabolism varies with gill morphology and myocardial bioenergetics in Gulf killifish

Bernard B. Rees[1,*], Jessica E. Reemeyer[2] and Brian A. Irving[3,4]

ABSTRACT

This study asked whether interindividual variation in maximum and standard aerobic metabolic rates of the Gulf killifish, *Fundulus grandis*, correlates with gill morphology and cardiac mitochondrial bioenergetics, traits reflecting critical steps in the O_2 transport cascade from the environment to the tissues. Maximum metabolic rate (MMR) was positively related to body mass, total gill filament length and myocardial oxygen consumption during maximum oxidative phosphorylation (multiple R^2=0.836). Standard metabolic rate (SMR) was positively related to body mass, total gill filament length and myocardial oxygen consumption during maximum electron transport system activity (multiple R^2=0.717). After controlling for body mass, individuals with longer gill filaments, summed over all gill arches, or greater cardiac respiratory capacity had higher whole-animal metabolic rates. The overall model fit and the explanatory power of individual predictor variables were better for MMR than for SMR, suggesting that gill morphology and myocardial bioenergetics are more important in determining active rather than resting metabolism. After accounting for body mass, heart ventricle mass was not related to variation in MMR or SMR, indicating that the quality of the heart (i.e. the capacity for mitochondrial metabolism) was more influential than heart size. Finally, the myocardial oxygen consumption required to offset the dissipation of the transmembrane proton gradient in the absence of ATP synthesis was not correlated with either MMR or SMR. The results support the idea that interindividual variation in aerobic metabolism, particularly MMR, is associated with variation in specific steps in the O_2 transport cascade.

KEY WORDS: *Fundulus*, Gill morphology, Heart, Metabolic rate, Mitochondria, Oxygen transport cascade

INTRODUCTION

Animal metabolic rates are complex phenotypes that reflect the flow of energy and materials through organisms, and they are essential features of animal physiology and ecology (Brown et al., 2004; Schmidt-Nielsen, 1997). Because most animals fuel the majority of their metabolism through the aerobic breakdown of macronutrients, the rate of oxygen consumption ($\dot{M}_{O_2}$) is a standard and reliable measure of metabolic rate (Schmidt-Nielsen, 1997). Much has been learned about the factors that influence $\dot{M}_{O_2}$ from studies of diverse species, populations and the effects of acclimation (McNab, 2002; Glazier, 2005; Schmidt-Nielsen, 1997). However, even when controlling ambient conditions and factors such as body size, activity, nutrition and reproductive status, the variation in $\dot{M}_{O_2}$ among individuals within a species or population is still substantial. In general, intraspecific variation in aerobic metabolism is repeatable, heritable and related to fitness. Because variation among individuals within a species reflects the raw material upon which natural selection acts, considerable attention has been given to understanding the proximate (mechanistic) and ultimate (evolutionary) causes of this variation (Bouchard et al., 1998; Burton et al., 2011; Careau and Garland, 2012; Crawford and Oleksiak, 2007; Glazier, 2005; Hoppeler, 2018; Killen et al., 2016; Konarzewski and Książek, 2013; Nespolo and Franco, 2007; Pettersen et al., 2018; Scott and Dalziel, 2021; White and Kearney, 2013).

When evaluating the causes and consequences of variation in aerobic metabolism, distinguishing between differences in metabolic rates due to activity is important. The upper limit of $\dot{M}_{O_2}$ by an animal is reflected in its maximum metabolic rate (MMR), typically measured during or immediately after vigorous exercise. During sustained aerobic exercise, oxygen utilization by tissues must be matched by oxygen uptake by the respiratory system and oxygen delivery by the circulatory system. Thus, studies of proximate causes of variation in MMR have examined various steps in the O_2 transport pathway from the environment to metabolically active tissues, where oxygen is ultimately consumed in mitochondrial oxidative phosphorylation. A large body of research has shown that the diffusing capacity of lungs or gills, cardiac output and the diffusing capacity of skeletal muscle vary among and within species as a function of body mass, 'athleticism', acclimatization or training, and habitat in a fashion that correlates with active $\dot{M}_{O_2}$ (Bassett and Howley, 2000; de Jager and Dekkers, 1975; Duncan, 2020; Glazier, 2005; Hillman et al., 2013; Hoppeler, 2018; Hughes, 1966; Killen et al., 2016; Scott and Dalziel, 2021; Wagner, 1996; Weibel et al., 2004, 1991; Weibel and Hoppeler, 2005). At the lower end of the $\dot{M}_{O_2}$ spectrum is that of a resting, post-absorptive, non-reproductive animal, known as the standard metabolic rate (SMR) for an ectothermic animal at a specified ambient temperature or the basal metabolic rate (BMR) for an endotherm within its thermoneutral zone (McNab, 1997). The $\dot{M}_{O_2}$ under these conditions is much less than MMR and, accordingly, the O_2 transport pathway is not likely to be limiting (Weibel et al., 1991). Rather, interspecific and intraspecific variation in SMR and BMR has been attributed to the mass or $\dot{M}_{O_2}$ of organs that are active in animals at rest (e.g. liver, brain, kidneys and heart) or constitute a large proportion of the body mass (e.g. skeletal muscle) (Burton et al., 2011; Killen et al., 2016; Konarzewski and Książek, 2013; Rolfe and Brown, 1997; White and Kearney, 2013).

The goal of the present study was to investigate the relationships between MMR and SMR and morphological and physiological variables related to the O_2 transport cascade in the Gulf killifish,

[1]Department of Biological Sciences, University of New Orleans, New Orleans, LA 70148, USA. [2]Department of Biology, McGill University, Montreal, QC, Canada H3A 1B1. [3]School of Kinesiology, Louisiana State University, Baton Rouge, LA 70803, USA. [4]Pennington Biomedical Research Center, Louisiana State University, Baton Rouge, LA 70808, USA.

*Author for correspondence (brees@uno.edu)

B.B.R., 0000-0001-5636-1700; J.E.R., 0000-0002-0081-2573

Received 15 October 2021; Accepted 27 May 2022

Journal of Experimental Biology (2022) 225, jeb243680. doi:10.1242/jeb.243680

List of symbols and abbreviations

AAS	absolute aerobic scope
AFL	average filament length
AIC_c	Akaike's information criterion, corrected for small sample size
ETS_{NS}	maximum electron transport system respiration with complex I and II substrates
FCR	flux control ratio
HRR	high-resolution respirometry
$LEAK_N$	leak respiration with complex I substrates
$LEAK_{NS}$	leak respiration with complex I and II substrates
M_b	body mass
MMR	maximum metabolic rate
$\dot{M}_{O_2}$	oxygen consumption rate
$OXPHOS_N$	phosphorylation-coupled respiration with complex I substrates
$OXPHOS_{NS}$	phosphorylation-coupled respiration with complex I and II substrates
RCR	respiratory control ratio
RMR	routine metabolic rate
ROX	residual oxygen consumption
SMR	standard metabolic rate
TFL	total filament length
TFN	total filament number

Fundulus grandis. *Fundulus grandis* is a small, ecologically dominant, teleost fish of the salt marshes of the Gulf of Mexico (Nordlie, 2006). Previous research on this species has demonstrated significant, repeatable, mass-independent variation in MMR and SMR among individuals held and measured under common garden conditions (Reemeyer and Rees, 2020; Virani and Rees, 2000). Our first objective was to determine whether individual variation in MMR is related to the initial steps of the O_2 transport cascade: the capacity for O_2 uptake and distribution. Although fish are the most speciose group of vertebrate animals and demonstrate marked variation in aerobic metabolism (Killen et al., 2016; Norin and Clark, 2016), the O_2 transport cascade in this group has received less attention than in terrestrial, air-breathing vertebrates (but see Scott and Dalziel, 2021; Steinhausen et al., 2008).

For water-breathing fish, the first step in the O_2 transport cascade is oxygen diffusion across the epithelium of the gill lamellae. The area available for gas exchange depends upon the area of individual lamellae, the density of lamellae on gill filaments, and the length and the total number of gill filaments projecting from the gill arches (Hughes, 1984). Interspecific comparisons have shown that total gill surface area tends to be greater in more active species than in less active species (Hughes, 1966; Killen et al., 2016; Palzenberger and Pohla, 1992). However, within species, the association between gill morphology and the capacity for aerobic metabolism is less clear. In the mummichog, *Fundulus heteroclitus*, population variation in gill surface area is positively correlated with the routine metabolic rate (RMR), a level of metabolism between SMR and MMR (McBryan et al., 2016). In laboratory-reared offspring from stream and marine populations of three-spined stickleback, corresponding to low and high MMR populations, respectively, the total gill filament length was greater in offspring from the high MMR marine population, although the difference in gill surface area was not significant (Dalziel et al., 2012). Conversely, more active, limnetic ecotypes of lake whitefish were found to have fewer gill filaments than less active, benthic ecotypes, just the opposite of what would be predicted if gill surface area was limiting aerobic metabolism (Laporte et al., 2016). These conflicting results could arise because fish gills serve multiple functions (Evans, 1980) and respond morphologically to diverse selective pressures (Chapman et al., 2008; Laporte et al., 2016). Importantly, the aforementioned studies evaluated trait differentiation among populations to infer the consequences of past evolution rather than testing whether variation in gill morphology among animals with similar evolutionary history affects their MMR. Here, we measured gill filament number, average filament length and total filament length as proxies of gill surface area (Chapman et al., 2008; Hughes, 1984; Palzenberger and Pohla, 1992). We predicted that these measures, either singly or together, would be positively correlated with MMR in *F. grandis* from a given location and held under similar laboratory conditions.

Once oxygen is taken up across the gills, it is circulated to the tissues by the heart and vascular system. According to the Fick principle, whole-animal $\dot{M}_{O_2}$ should increase with increasing cardiac output (the product of stroke volume and heart rate) for a given arterio-venous oxygen difference. Indeed, increased $\dot{M}_{O_2}$ of Atlantic cod during exercise is linearly related to cardiac output (Webber et al., 1998). Moreover, intraspecific variation in the capacity to elevate $\dot{M}_{O_2}$ during swimming in rainbow trout is associated with greater cardiac output *in vivo* and greater power generation by hearts *in vitro* (Claireaux et al., 2005). Because cardiac power generation requires ATP and is directly correlated with $\dot{M}_{O_2}$ by the heart itself (Farrell and Smith, 2017), we hypothesized that variation in the capacity for cardiac mitochondrial metabolism should be reflected by variation in MMR. This expectation is partly supported by measurements of enzyme activity in fish hearts. In Atlantic cod, intraspecific variation in $\dot{M}_{O_2}$ during swimming is positively correlated with the ventricular activity of cytochrome *c* oxidase, the terminal enzyme of the electron transport system (Sylvestre et al., 2007). In contrast, variation in aerobic activity among populations of three-spined stickleback or ecotypes of lake whitefish was not paralleled by changes in the ventricular activity of cytochrome *c* oxidase and citrate synthase, a marker of citric acid cycle activity (Dalziel et al., 2012, 2015). To directly test the hypothesis that cardiac mitochondrial metabolism is correlated with MMR within a population, we used high-resolution respirometry (HRR) to measure mitochondrial $\dot{M}_{O_2}$ by permeabilized myocardial tissue (Doerrier et al., 2018; Kuznetsov et al., 2008; Pesta and Gnaiger, 2012; Veksler et al., 1987). By the controlled addition of substrates and inhibitors, HRR affords the opportunity to probe various steps of mitochondrial oxidative phosphorylation in preparations that preserve some cellular structure. Moreover, HRR can differentiate $\dot{M}_{O_2}$ due to ATP synthesis by oxidative phosphorylation (OXPHOS) from that required to offset the dissipation of the transmembrane proton gradient in the absence of ATP synthesis (LEAK). We predicted that $\dot{M}_{O_2}$ coupled to ATP synthesis by permeabilized myocardial tissue would be positively related to MMR in *F. grandis* from a given location and held under similar laboratory conditions.

The second objective of this study was to determine whether individual variation in SMR was correlated with these same gill and heart variables. Although the O_2 transport cascade is not expected to limit oxygen uptake by animals at rest (see above), several observations suggest that traits related to O_2 uptake and transport are associated with resting $\dot{M}_{O_2}$. Gillooly et al. (2016) demonstrated a strong positive relationship between the respiratory diffusing capacity of lungs and gills and RMR or BMR across a broad range of vertebrates. Also, as mentioned above, in populations of *F. heteroclitus*, gill surface area is positively associated with RMR, a measure of metabolism that is close to SMR, but includes some low, indeterminant level of activity. Furthermore, Jayasundara et al.

(2015) showed that $\dot{M}_{O_2}$ by intact hearts was correlated with RMR across five species, and Drown et al. (2021) recently showed that the $\dot{M}_{O_2}$ of whole hearts is positively correlated with SMR in *F. heteroclitus*, albeit under specific acclimation conditions and only with certain metabolic substrates. Also, LEAK respiration may contribute to interindividual variation in BMR in mammals or SMR in fish (Rolfe and Brown, 1997; Salin et al., 2016; but see Larsen et al., 2011). While this effect is likely to be most relevant for large organs (e.g. liver and skeletal muscle), the contribution of cardiac LEAK respiration to whole-animal $\dot{M}_{O_2}$ is unknown. Because the predicted outcomes of this second objective were less certain, we adopted the null hypothesis (no relationship) for this objective.

MATERIALS AND METHODS

Fish collection and husbandry

Gulf killifish, *Fundulus grandis* Baird and Girard 1853 (n=39; mean mass 5.71 g, range 3.73–9.51 g at the time of experiments), were collected from the Grand Bay National Estuarine Research Reserve in August 2018. These fish were maintained and used between August 2018 and May 2019, as described in Reemeyer and Rees (2020), after which they were held for an additional 6 weeks on a 12 h:12 h light:dark photoperiod in filtered, aerated and dechlorinated municipal water made to a salinity of 9–12 using artificial sea salt (Instant Ocean) at 25°C. Fish were fed dried flake food (TetraMin) once per day. Food was withheld for 24 h before whole-animal respirometry or euthanasia for tissue sampling. All procedures on live animals were approved by the University of New Orleans Institutional Animal Care and Use Committee.

Whole-animal respirometry

Fish used in this study were previously subjected to intermittent-flow respirometry (Svendsen et al., 2016), as described in Reemeyer and Rees (2020). For the current study, the same procedures were repeated to determine MMR and SMR within 2 weeks of euthanasia for tissue harvesting (see below). To induce MMR, fish were chased individually by hand to exhaustion (3 min) and immediately transferred to the respirometer (<30 s). Consistent with previous observations (Reemeyer and Rees, 2020), the highest $\dot{M}_{O_2}$ for many fish occurred several hours after chasing. For only 8 fish was $\dot{M}_{O_2}$ highest immediately following chasing: 25 fish displayed their highest $\dot{M}_{O_2}$ when the room lights went out (ca. 4 h later); 3 had their highest $\dot{M}_{O_2}$ when the lights came on the next morning; and 3 had their highest $\dot{M}_{O_2}$ at some other time during the respirometry trials. These rates were up to 77% higher than the $\dot{M}_{O_2}$ measured immediately after chasing (average 35% higher). Accordingly, the measurement interval with the highest $\dot{M}_{O_2}$ over the entire respirometry trial (ca. 20 h) was retained for analysis. In addition, we used the iterative slope analysis described by Zhang et al. (2020) to ensure that we captured the highest reliable $\dot{M}_{O_2}$ for each fish. In brief, for the retained measurement intervals, which were 2 min long during the first hour after chasing and 4 min thereafter, the slope of oxygen concentration versus time was determined over all possible periods of 30, 60, 90 and 120 s, each advancing by 1 s (Zhang et al., 2020). As reported elsewhere (Zhang et al., 2020), a period of 60 s resulted in statistically higher $\dot{M}_{O_2}$ than those estimated over the entire measurement interval (average increase 11%), while still achieving high coefficients of determination from least-squares linear regression (average r^2>0.98). SMR was determined as the 20% quantile of all $\dot{M}_{O_2}$ measurements collected between 20:00 h and 06:00 h during a given trial (Chabot et al., 2016; Reemeyer and Rees, 2020). All $\dot{M}_{O_2}$ data were corrected for microbial respiration as previously described (Reemeyer and Rees, 2020).

Tissue sampling and gill morphometrics

Fish were euthanized by rapid chilling followed by cervical transection (Larter and Rees, 2017), and heart ventricles were quickly dissected (<2 min) and placed in 1 ml relaxing and biopsy preservation solution (BIOPS, in mmol l^{-1}: 50 K^+-MES, 20 taurine, 0.5 dithiothreitol, 6.56 $MgCl_2$, 5.77 ATP, 15 phosphocreatine, 2.77 CaK_2 EGTA, 7.23 K_2 EGTA and 20 imidazole, adjusted with 5 mol l^{-1} KOH to pH 7.1 at 0°C; Pesta and Gnaiger, 2012) on ice. Hearts were held at 0–2°C for 1 or 2 days prior to determination of myocardial $\dot{M}_{O_2}$ (see Supplementary Materials and Methods). Immediately after the removal of the heart, the right gill basket was removed. Individual gill arches were dissected, fixed overnight in neutral buffered formalin (4% formaldehyde, 33 mmol l^{-1} NaH_2PO_4, 46 mmol l^{-1} Na_2HPO_4), and kept in 100% ethanol. Total filament number (TFN), average filament length (AFL) and total filament length (TFL) were determined as described previously (Rees and Matute, 2018).

High-resolution respirometry of permeabilized myocardial tissue

Intact heart ventricles were weighed and prepared for high-resolution respirometry following protocols for permeabilized human skeletal muscle fibers (Doerrier et al., 2018; Pesta and Gnaiger, 2012) with minor modification (see Supplementary Materials and Methods). Permeabilized myocardial tissue, roughly corresponding to one-quarter to one-half of the ventricle mass (mean mass 1.25±0.41 mg, range 0.64–2.32 mg), was transferred to the chamber of an Oroboros O2k respirometer (Oroboros Instruments) containing 2.0 ml MiR05 respirometry medium (in mmol l^{-1}: 110 sucrose, 60 K^+-lactobionate, 0.5 EGTA, 3 $MgCl_2$, 20 taurine, 10 KH_2PO_4, 20 Hepes adjusted to pH 7.15 with KOH at 25°C, with 1 g l^{-1} essentially fatty acid free BSA; Pesta and Gnaiger, 2012), supplemented with 20 mmol l^{-1} creatine and 25 µmol l^{-1} blebbistatin. Myocardial tissue respiration was measured at 25°C using a substrate–uncoupler–inhibitor titration (SUIT) modified from previous studies of fish heart metabolism (Fig. 1) (Baris et al., 2016; Iftikar and Hickey, 2013). The titration and corresponding respiratory states followed the sequence: NADH-generating substrates (5 mmol l^{-1} pyruvate, 2 mmol l^{-1} malate and 10 mmol l^{-1} glutamate) to measure leak respiration due to complex I activity ($LEAK_N$); 5 mmol l^{-1} ADP to stimulate phosphorylation-coupled respiration due to complex I activity; 10 µmol l^{-1} cytochrome *c* to check the integrity of the outer mitochondrial membrane ($OXPHOS_N$); 10 mmol l^{-1} succinate to saturate complex II ($OXPHOS_{NS}$); 0.5 µmol l^{-1} oligomycin to inhibit ATP synthesis to measure leak respiration due to complex I and complex II activity ($LEAK_{NS}$); carbonyl cyanide *m*-chlorophenyl hydrazone (CCCP), in steps of 0.5 µmol l^{-1}, to uncouple mitochondria and elicit maximum electron transport system activity (ETS_{NS}); and 2.5 µmol l^{-1} antimycin A to completely inhibit respiration due to mitochondrial electron transport and measure residual oxygen flux (ROX). The assay medium was gassed with pure oxygen as needed to keep the oxygen concentration between 120 and 400 µmol l^{-1}. Data acquisition, rate analyses and instrument calibration were performed with DatLab, version 7 (Oroboros Instruments) as previously described (Doerrier et al., 2018; Pesta and Gnaiger, 2012). Up to four O2k respirometers were used at a time (eight chambers), allowing the simultaneous measurement of four hearts in duplicate.

Pilot experiments were conducted to validate the use of ventricles after storage in BIOPS at 0–2°C for up to 2 days, along with validation of uncoupler and substrate concentrations (Supplementary Materials and Methods, Table S1, Figs S1–S4). Of

Journal of Experimental Biology (2022) 225, jeb243680. doi:10.1242/jeb.243680

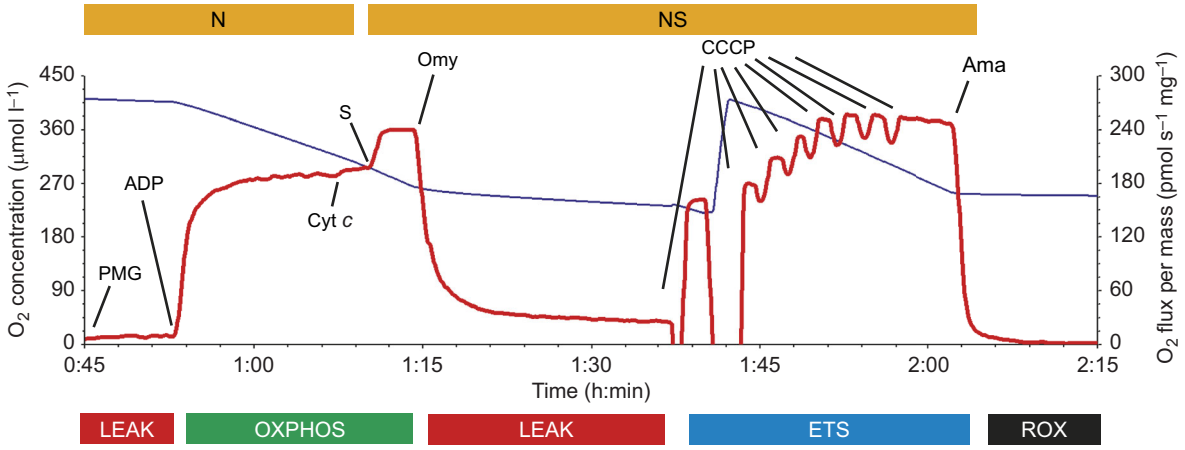

Fig. 1. Example measurement of mitochondrial respiration by *Fundulus grandis* myocardial tissue. A representative high-resolution respirometry assay of *F. grandis* permeabilized myocardial tissue (1.11 mg tissue, 25°C) showing oxygen concentration (blue) and oxygen flux (red). Respiratory substrates are indicated at the top, where N represents NADH-generating substrates to saturate complex I (pyruvate, malate and glutamate; PMG) and NS indicates the further addition of succinate (S) to saturate complex II. Respiratory states are indicated at the bottom, where LEAK corresponds to the oxygen flux before the addition of ADP or after inhibition of ATP synthase by oligomycin (Omy); OXPHOS is oxygen flux in the presence of ADP; ETS is the maximum uncoupled oxygen flux, determined by the stepwise addition of carbonyl cyanide *m*-chlorophenyl hydrazone (CCCP); and ROX is the residual oxygen flux after the addition of antimycin A (Ama). Cyt *c*, cytochrome *c*.

the 39 fish used in the main study, ventricles from 22 fish were permeabilized and assayed after 1 day of storage, and ventricles from 17 fish were permeabilized and assayed after 2 days of storage. As observed in the pilot experiments, there was no significant effect of time stored at 0–2°C on any metric of mitochondrial performance (P>0.15 for all rates, flux control ratios and cytochrome *c* effects). Accordingly, data from all preparations were pooled without regard for the time ventricles were stored in BIOPS.

In addition, for a given ventricle, variation between oxygen flux determinations of duplicate permeabilized preparations was low: the coefficient of variation between duplicates averaged 11–12% for $\dot{M}_{O_2}$ during oxidative phosphorylation and maximum electron transport system activity ($OXPHOS_{NS}$ and ETS_{NS}, respectively). In 8 out of 78 total replicates, however, one replicate assay had much lower oxygen flux (<50%), slower kinetics and higher noise than the other replicate from the same heart. This included two replicates for which the addition of 10 µmol l^{-1} cytochrome *c* resulted in >20% increase in $OXPHOS_N$ respiration, indicating damage to the outer mitochondrial membrane, likely arising from tissue dissection and permeabilization (see Supplementary Materials and Methods). The respiratory control ratios (RCR, $OXPHOS_{NS}/LEAK_{NS}$) for these replicates (4.2±1.1, mean±s.d., n=8) were significantly lower (P=0.001, paired t-test) than the RCR for the other replicates from the same hearts (10.3±2.5, mean±s.d., n=8), indicating poorly coupled mitochondria. These replicates were removed from the analyses. In addition, the ventricle of one of the smaller fish yielded only one sample of myocardial tissue >0.5 mg. Thus, oxygen flux was from a single ventricle preparation for nine fish. For the remaining 30 fish, oxygen flux from duplicate ventricle preparations was averaged and considered a single determination for statistical analyses.

Statistics

General linear modeling was used to assess the relationship between whole-animal aerobic metabolism, gill morphology and myocardial $\dot{M}_{O_2}$. Separate models were fitted for MMR and SMR with body mass, ventricle mass, TFL, $LEAK_N$, $LEAK_{NS}$, $OXPHOS_N$, $OXPHOS_{NS}$ and ETS_{NS} as predictor variables. Including body mass in the models simultaneously accounted for mass effects on whole-animal $\dot{M}_{O_2}$, as well as on other predictor variables, such that all reported results are independent of variation in body mass among individuals. Variables were $\log_{10}$ transformed prior to analysis because of the known allometric relationships of metabolic and morphological data, although analyses of untransformed data yielded essentially identical results. All predictor variables were included in the initial models, and individual variables were removed in a stepwise fashion when doing so improved model fit, as judged by a decrease in Akaike's information criterion, corrected for small sample size (AIC_c) (Burnham and Anderson, 2002). The strength of the evidence supporting the final models was determined as the ratio of their Akaike weight to that of competing models. Visualization of the relationships between specific predictor variables and either MMR or SMR and the determination of Pearson's correlation coefficients used mass-independent residuals of ordinary least-squares linear regression of log–log plots of the variables of interest and body mass. Although the fish used in this study included both male and female fish collected from two nearby drainages, initial analyses of variance showed that neither sex nor collection site affected any metabolic or morphological variable, consistent with previous work on this cohort (Reemeyer and Rees, 2020). Thus, fish sex and collection site were not included in these models. Analyses were performed in GraphPad Prism, v.7.01, and SYSTAT, v.13. Data collected during this study are available from Dryad (doi:10.5061/dryad.jsxksn0bx).

RESULTS

This study aimed to determine whether variation in MMR and SMR by the Gulf killifish, *F. grandis*, held under common-garden conditions correlates with steps in the O_2 transport cascade from the environment to the tissues. As expected, MMR, SMR, gill morphology and heart size were strongly influenced by body mass (Table 1). Nevertheless, considerable variation remained after accounting for body size. In particular, mass-specific MMR and SMR varied approximately 2-fold (mean mass-specific MMR 0.336 µmol g^{-1} min^{-1}, range 0.222–0.437 µmol g^{-1} min^{-1}; mean mass-specific SMR 0.073 µmol g^{-1} min^{-1}, range 0.052–0.106 µmol g^{-1} min^{-1}). We asked whether the variation in MMR and SMR not accounted for by body size could be explained by

Journal of Experimental Biology (2022) 225, jeb243680. doi:10.1242/jeb.243680

Table 1. Mean, variation and allometric relationships of whole-animal aerobic metabolism, ventricle mass and gill morphology in a cohort of Gulf killifish, *Fundulus grandis*

Variable	Mean	Range	CV (%)	*a* [95% CI]	*b* [95% CI]	r^2
MMR (μmol min^{-1})	1.92	1.05–3.46	29.6	−0.56 [−0.73– −0.39]	1.11 [0.88–1.33]	0.733
SMR (μmol min^{-1})	0.42	0.21–0.68	25.8	−1.07 [−1.26– −0.89]	0.91 [0.67–1.16]	0.608
M_v (mg)	5.95	3.55–9.99	27.7	0.149 [−0.06–0.36]	0.82 [0.54–1.10]	0.492
AFL (mm)	1.32	1.06–1.67	10.3	−0.16 [−0.22– −0.10]	0.37 [0.29–0.46]	0.682
TFN	882	754–1042	8.0	2.80 [2.72–2.88]	0.19 [0.09–0.29]	0.288
TFL (mm)	1170	809–1561	15.8	2.64 [2.54–2.74]	0.57 [0.43–0.70]	0.652

Allometric constants are from ordinary least-squares linear regression of the equation $\log_{10}(y)=a+b\times\log_{10}(M_b)$, where y is the variable of interest and M_b is total body mass. Constants *a* and *b* are shown with their 95% confidence interval, CI (n=39). All coefficients of determination (r^2) were statistically significant (P<0.001). CV, coefficient of variation; MMR, maximum metabolic rate; SMR, standard metabolic rate; M_v, ventricular mass; AFL, average filament length; TFN, total filament number; TFL, total filament length.

size-adjusted gill morphology, ventricle mass or myocardial mitochondrial metabolism.

Protocols for tissue storage, cell permeabilization and high-resolution respirometry of myocardial mitochondria were optimized (Supplementary Materials and Methods, Table S1, Figs S1–S4) and used to determine $\dot{M}_{O_2}$ by ventricular tissue in various respiratory states. Oxygen flux in the LEAK state with complex I (PMG) and complex II (PMGS) substrates was low, whereas oxygen flux upon addition of ADP (OXPHOS) was high and sustained (Fig. 1, Table 2). The RCR (OXPHOS/LEAK) is commonly used to assess the quality of mitochondria. The RCR averaged 9.2±2.4 (mean ±s.d.) with complex I and II substrates, indicating well-coupled mitochondria. Moreover, the addition of cytochrome *c* only had a small stimulatory effect on $OXPHOS_N$ (5.7±3.7% increase, mean ±s.d.), indicating minimal damage to the outer mitochondrial membrane. Finally, OXPHOS respiration with complex I and II substrates ($OXPHOS_{NS}$) routinely exceeded 90% of the oxygen flux during maximum electron transport capacity (ETS_{NS}). These characteristics of mitochondrial respiration are consistent with high-quality myocardial mitochondria.

While variation between replicate oxygen flux determinations for a given individual was low (see Materials and Methods), there was considerable variation in myocardial $\dot{M}_{O_2}$ among individuals in all respiratory states (Table 2). This variation was of similar magnitude to the individual variation in mass-specific MMR and SMR. For example, $OXPHOS_{NS}$ and ETS_{NS} varied from 1.5- to 1.6-fold among fish. This variation was also evident in the flux control ratio (FCR) (Table 2), which standardizes the $\dot{M}_{O_2}$ in each state by the $\dot{M}_{O_2}$ during maximum electron transport system activity (e.g. 1.6-fold variation in FCR for $OXPHOS_{NS}$). Oxygen flux expressed per milligram of permeabilized ventricular tissue was independent of body mass (r^2<0.03 for all respiratory states). Values of $\dot{M}_{O_2}$ for intact ventricles in each respiratory state, calculated as the product of respiration rate per milligram of tissue and ventricle mass, were positively related to body mass, which was a direct consequence of the strong allometric relationship of ventricular mass (Table 1).

General linear modeling was used to determine whether variation in whole-animal MMR and SMR was explained by variation in gill morphology, ventricular mass or myocardial bioenergetics (Table 3). Body mass was included in these models because of its strong effects on metabolic and morphological variables. The best model describing variation in MMR included body mass, TFL and myocardial $\dot{M}_{O_2}$ during oxidative phosphorylation with complex I and complex II substrates ($OXPHOS_{NS}$). The ΔAIC for this model was 1.60 compared with the next-best model. The corresponding Akaike weights indicated the final model was >2.2 times more likely to describe the MMR data than competing models (Table S2). The best model describing variation in SMR included body mass, TFL and myocardial $\dot{M}_{O_2}$ during maximum electron transport system activity (ETS_{NS}). It should be noted that the final model describing variation in SMR was only marginally better (ca. 1.4 times more likely) than models that retained ventricle mass (ΔAIC=0.65) or excluded ETS_{NS} (ΔAIC=0.70) (Table S2). Nevertheless, the final models explained 84% and 72% of the variation in MMR and SMR, respectively.

The correlations between MMR and SMR and the explanatory predictor variables are shown in Fig. 2. The correlations were highest for body mass (Fig. 2A,B), followed by TFL (Fig. 2C,D) and myocardial $\dot{M}_{O_2}$ (Fig. 2E,F). The effects of TFL and myocardial $\dot{M}_{O_2}$ are presented as mass-independent residuals of least-squares linear regression of $\log_{10}$ of the indicated variable with $\log_{10}$ body mass. After accounting for the effects of body mass, variation in TFL explained approximately 30% of the variation in MMR, whereas variation in myocardial $OXPHOS_{NS}$ explained 13% of the variation in MMR. However, variation in TFL explained only 21%, and variation in myocardial ETS_{NS} only 7%, of the mass-independent variation in SMR.

Table 2. Oxygen flux and flux control ratios for *F. grandis* permeabilized myocardial tissue

	Oxygen flux (pmol s^{-1} mg^{-1})			Flux control ratio		
Respiratory state	Mean±s.d.	Range	CV (%)	Mean±s.d.	Range	CV (%)
$LEAK_N$	8±3	2–18	37.6	0.033±0.012	0.009–0.069	35.4
$OXPHOS_N$	182±22	145–227	12.0	0.747±0.065	0.609–0.931	8.7
$LEAK_{NS}$	26±5	18–40	20.5	0.109±0.022	0.075–0.162	20.4
$OXPHOS_{NS}$	232±27	187–288	11.8	0.955±0.089	0.737–1.190	9.4
ETS_{NS}	244±28	197–311	11.3	–	–	–

$LEAK_N$, LEAK respiration with complex I substrates (pyruvate, malate and glutamate); $OXPHOS_N$, phosphorylation-coupled respiration with complex I substrates; $LEAK_{NS}$, LEAK respiration with complex I and II substrates (pyruvate, malate, glutamate and succinate); $OXPHOS_{NS}$, phosphorylation-coupled respiration with complex I and II substrates; ETS_{NS}, maximum uncoupled electron transport system respiration with complex I and II substrates. Flux control ratios were determined as the oxygen flux measured in each respiratory state divided by ETS_{NS} for a given preparation. All measurements were made at 25°C and corrected for residual oxygen consumption (n=39).

Journal of Experimental Biology (2022) 225, jeb243680. doi:10.1242/jeb.243680

Table 3. Results of general linear modeling of the effects of morphological and myocardial bioenergetic variables on MMR and SMR of *F. grandis*

	Estimate	s.e.	*P*
MMR (μmol min^{-1})			
Constant	−3.676	0.666	<0.001
β M_b	0.664	0.152	<0.001
β TFL	0.831	0.216	<0.001
β $OXPHOS_{NS}$	0.381	0.170	0.032
Multiple R^2	0.836		
ΔAIC_c	1.60		
SMR (μmol min^{-1})			
Constant	−4.143	0.846	<0.001
β M_b	0.477	0.179	0.012
β TFL	0.817	0.254	0.003
β ETS_{NS}	0.374	0.211	0.086
Multiple R^2	0.717		
ΔAIC_c	0.65		

Intercepts, coefficients (β), R^2 and the ΔAIC_c of the final models are shown. Variables were $\log_{10}$ transformed. See Table S2 for comparison with other models. ΔAIC_c, the decrease in Akaike's information criterion of the best model, corrected for small sample size, compared with the next-best model; MMR, maximum metabolic rate; SMR, standard metabolic rate; M_b, body mass; TFL, total filament length; $OXPHOS_{NS}$, phosphorylation-coupled respiration with complex I and II substrates; ETS_{NS}, maximum uncoupled electron transport system respiration with complex I and II substrates.

Given that total filament length (TFL) is the product of total filament number (TFN) and average filament length (AFL), the relationships between mass-independent variation in MMR and TFN and AFL were assessed. After accounting for the effects of body mass, both TFN and AFL were positively correlated with MMR (Fig. 3), suggesting that increases in both component variables are associated with higher MMR. Interestingly, ventricle mass was not retained in the final models describing variation in MMR or SMR. This is probably because ventricle mass is highly correlated with body mass and did not explain any variation in MMR or SMR other than that explained by body size.

Finally, general linear modeling was also performed on mass-specific MMR and SMR and on data without logarithmic transformation. These analyses yielded final models that retained the same predictor variables for MMR and SMR as shown in Table 3. In addition, analyses of the variation in absolute aerobic scope (AAS), the difference between MMR and SMR, yielded essentially identical results to those shown for MMR (Table S2). This was expected because variation in MMR is quantitatively more important than that in SMR in determining the AAS in this species (Reemeyer and Rees, 2020).

DISCUSSION

Here, we demonstrate that interindividual variation in MMR and SMR of Gulf killifish, *Fundulus grandis*, correlates with variation in gill morphology and myocardial bioenergetics. These relationships were observed among individuals collected from a given location, held under common garden conditions, and after accounting for variation in body mass. Thus, the current study complements and extends earlier interspecific, interpopulation and acclimation studies on the relationship between the O_2 transport cascade and animal aerobic metabolism.

Correlates of MMR

We found that within a given cohort of *F. grandis*, variation in TFL was positively correlated with MMR (Table 3). After mass correction, variation in TFL explained 30% of the variation in MMR (Fig. 2), which was accounted for by increases in filament number and the length of individual filaments (Fig. 3). It is important to note that TFL is only a proxy of gill surface area, albeit one that is commonly used (Palzenberger and Pohla, 1992) and validated by parallel measurements of TFL and gill surface area in other species (Chapman et al., 2008). Hence, the current results support the hypothesis that variation in gill surface area is linked to variation in maximum $\dot{M}_{O_2}$ among individuals within a species.

Our results largely agree with comparisons among species of fish that have shown that more-active species generally have larger gills than less-active species, and that this variation correlates with differences in whole-animal $\dot{M}_{O_2}$ (de Jager and Dekkers, 1975; Duncan, 2020; Hughes, 1966; Palzenberger and Pohla, 1992; Killen et al., 2016). In studies of population variation, however, the relationship between gill surface area and whole-animal $\dot{M}_{O_2}$ is less clear: some studies have shown a positive relationship between gill surface area and aerobic metabolism (McBryan et al., 2016), whereas other studies show no relationship, or even a negative relationship, when comparing populations or ecotypes having different levels of aerobic activity (Dalziel et al., 2012; Laporte et al., 2016). An important factor contributing to the divergence of gill morphology is the ambient oxygen level, where species or populations experiencing hypoxia typically have larger gills (Chapman et al., 2002, 2008). Accordingly, Laporte et al. (2016) proposed that the larger gill surface area in a less-active, benthic ecotype of lake whitefish compared with a more-active, limnetic ecotype was a response to the lower oxygen that the benthic ecotype faces in nature, rather than a consequence of differing levels of aerobic activity. Thus, comparisons among species or populations assess the consequences of past selection, genetic drift and other processes, while studies on individuals from similar environments and having similar evolutionary histories (such as the current one) can illuminate the range of variation upon which selection may act in the future.

We also showed that interindividual variation in MMR by *F. grandis* was positively correlated with the maximum ATP-generating respiration ($OXPHOS_{NS}$) by myocardial mitochondria (Table 3). In particular, variation in $OXPHOS_{NS}$ explained 13% of the mass-independent variation in MMR (Fig. 2). Because the heart's capacity to pump blood through the circulation is supported by aerobic metabolism, at least under conditions of normal oxygenation (Farrell and Smith, 2017), it stands to reason that whole-animal $\dot{M}_{O_2}$ might vary with the capacity for myocardial oxidative phosphorylation. While the connection between cardiac energy metabolism and mechanical performance has long been appreciated (Driedzic and Gesser, 1994; Farrell and Smith, 2017; Moyes, 1996; Rodnick and Gesser, 2017), the current results extend this link to an organismal trait, maximum whole-animal aerobic metabolism.

Because the heart ventricles used in this study were approximately 0.1% of the total body mass (Table 1), we do not attribute the positive relationship between $OXPHOS_{NS}$ and MMR to the quantitative contribution of ventricular $\dot{M}_{O_2}$ to whole-animal $\dot{M}_{O_2}$. The $\dot{M}_{O_2}$ of a ventricle of average mass (5.95 mg) having an average rate of $OXPHOS_{NS}$ respiration (232 pmol mg^{-1} s^{-1}) represents only 4.3% of the average MMR (1.92 μmol min^{-1}), a value that falls within the range reported for other species (Farrell and Smith, 2017). Variation among individuals within this small fraction of MMR cannot explain the overall variation we measured in MMR. Instead, we propose that the relationship between myocardial $OXPHOS_{NS}$ and MMR is due to the requirement for mitochondrial ATP production to sustain cardiac output and support

Journal of Experimental Biology (2022) 225, jeb243680. doi:10.1242/jeb.243680

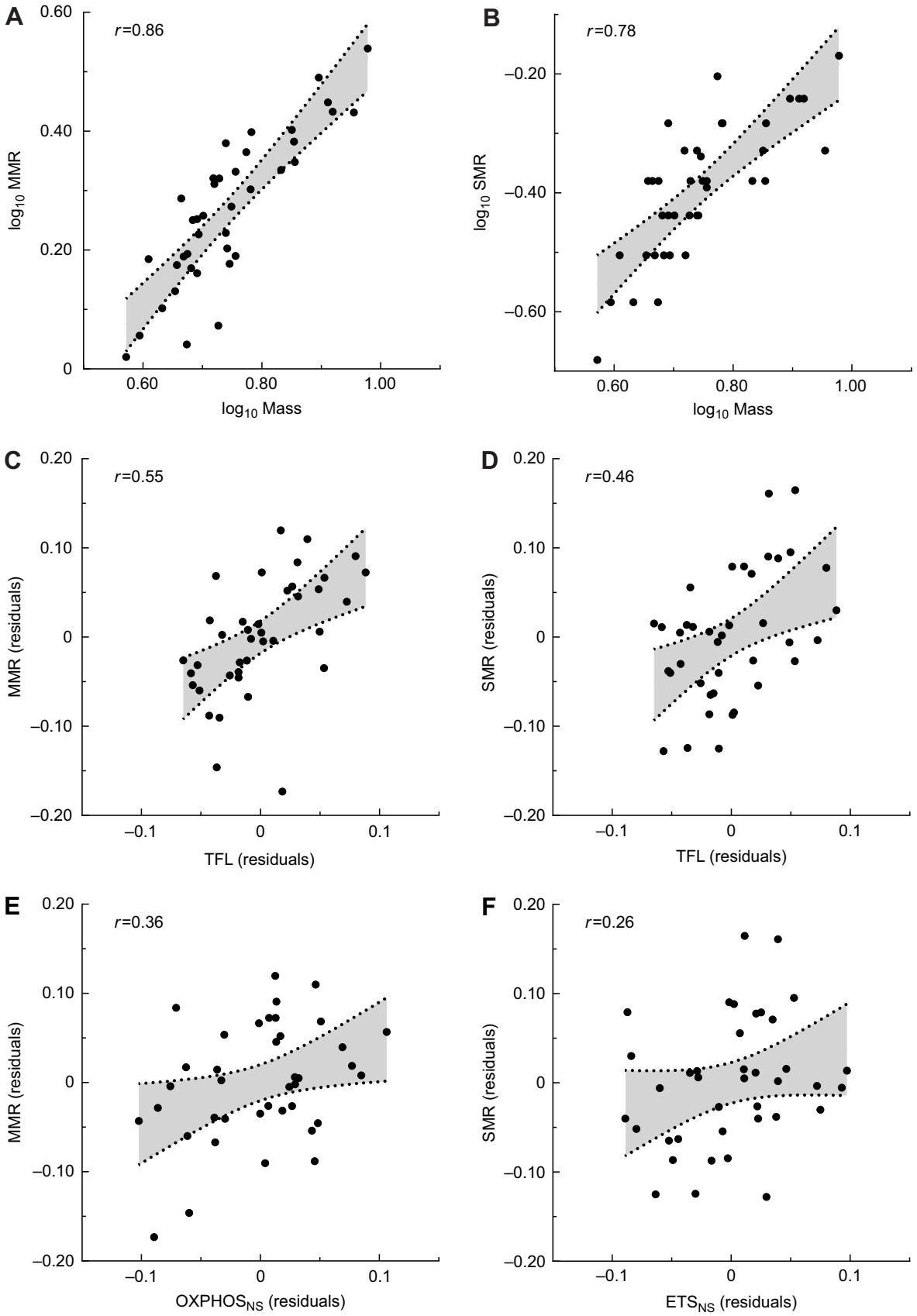

Fig. 2. Interindividual variation in aerobic metabolism of *F. grandis* correlates with morphological and myocardial variables. The relationships of maximum metabolic rate (MMR) and standard metabolic rate (SMR) with body mass (A,B), total gill filament length (TFL; C,D) and myocardial $\dot{M}_{O_2}$ ($OXPHOS_{NS}$ and ETS_{NS}; E,F). For C–F, mass-independent residuals of least-squares linear regression of $\log_{10}$ of the indicated variable with $\log_{10}$ body mass are plotted. The 95% confidence intervals (shaded) and Pearson's correlation coefficients (*r*) are from least-squares linear regressions for *n*=39 fish. See Table 3 for overall model fit statistics.

Journal of Experimental Biology (2022) 225, jeb243680. doi:10.1242/jeb.243680

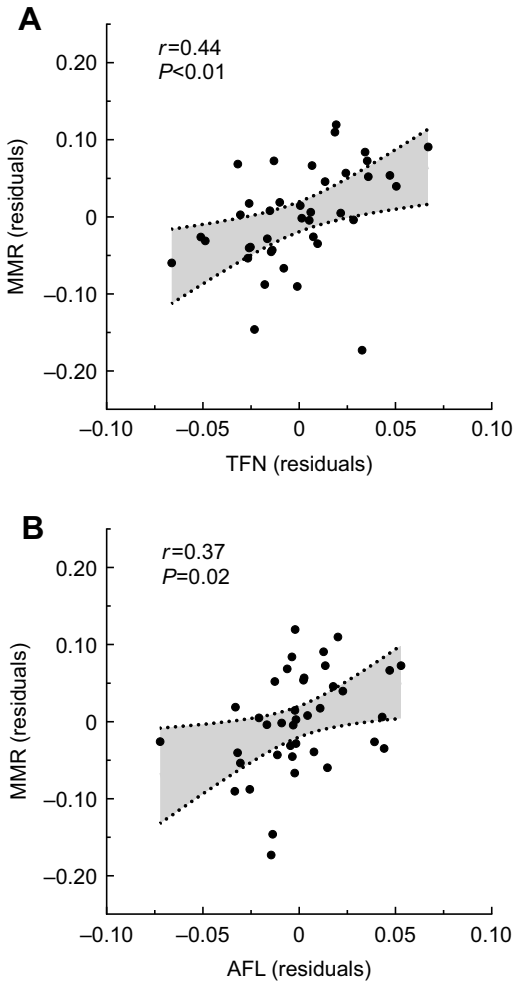

Fig. 3. Correlation between MMR and gill morphology in *F. grandis*. The relationships of MMR with total filament number (TFN; A) and average filament length (AFL; B). Mass-independent residuals of least-squares linear regression of $\log_{10}$ of the indicated variable with $\log_{10}$ body mass are plotted. The 95% confidence intervals (shaded) and Pearson's correlation coefficients (*r*) and *P*-values are from least-squares linear regressions for *n*=39 fish.

oxygen delivery to the tissues. Given that myocardial $\dot{M}_{O_2}$ is linearly related to cardiac power generation (Farrell and Smith, 2017), the 1.5-fold variation we observed in myocardial $OXPHOS_{NS}$ could translate to an equally large effect on cardiac power generation. Using the conversion factor of 0.3 µl O_2 s^{-1} mW^{-1} g^{-1} ventricular mass (Farrell and Smith, 2017), the range of $OXPHOS_{NS}$ respiration measured here corresponds to a range in cardiac power of 14–21 mW g^{-1}, comparable to the power generated by isolated fish hearts in normal oxygen conditions at similar temperatures (Farrell and Smith, 2017; Rodnick and Gesser, 2017).

The variation in myocardial mitochondrial respiration reported here could arise from variation in mitochondrial quantity, quality or both. Mitochondrial density in skeletal muscle has been proposed to be a major determinant of MMR among mammals differing in body size, lifestyle and training (Weibel et al., 2004; Weibel and Hoppeler, 2005). However, Jacobs and Lundby (2013) argued that training-induced increases in MMR in humans involve both increased mitochondrial density and increased capacity for oxidative phosphorylation per mitochondria. Similarly, differences in muscle mitochondrial respiration in populations of deer mice living at different elevations correlate with increased mitochondrial density, altered intracellular mitochondrial distribution and greater surface area of cristae (Mahalingam et al., 2017). Factors that could impact the OXPHOS capacity of mitochondria include altered expression of mitochondrial enzymes (Oleksiak et al., 2005) or their interactions with membrane lipids; in particular, cardiolipin (Lau et al., 2017; Moyes and Hood, 2003; Paradies et al., 2014). Further research is needed to fully elucidate the molecular bases of interindividual variation in myocardial aerobic metabolism in fish and in animals in general.

As mentioned above, it is well established that variation in the capacity for mitochondrial metabolism of skeletal muscle is linked to interspecific and intraspecific variation in MMR (Karakelides et al., 2010; Hoppeler, 2018; Jacobs and Lundby, 2013; Scott and Dalziel, 2021; Weibel et al., 1991, 2004; Weibel and Hoppeler, 2005). This association follows from the observation that skeletal muscle may account for as much as 90% of the oxygen consumed during exercise (Hoppeler, 2018). Thus, an intriguing possibility is that certain individuals have a greater capacity for mitochondrial respiration in both heart and skeletal muscle, the former in support of cardiac output and the latter in support of elevated locomotor activity. In humans, exercise training, age and disease affect mitochondrial content or respiratory capacity of skeletal muscle and potentially other organs (Memme et al., 2021), suggesting that mitochondrial function of several tissues may vary in a coordinated fashion among individuals.

Given that cardiac output is the product of heart rate and stroke volume, the latter of which is influenced by heart size, it was surprising, perhaps, that variation in ventricle mass was not related to variation in MMR, after accounting for body mass. In mammals, the increase in maximum $\dot{M}_{O_2}$ due to training is associated with increased heart mass (Bassett and Howley, 2000), 'athletic' species have larger hearts than sedentary species of the same body size (Hoppeler and Weibel, 1998), and individual variation in MMR of mice is correlated with ventricle mass (Rezende et al., 2006). Among fishes, population and ecotype variation in aerobic metabolism has been positively correlated with body mass-adjusted ventricle mass in three-spined stickleback, lake whitefish and sockeye salmon (Dalziel et al., 2015, 2012; Eliason et al., 2011). In Trinidadian guppies, in contrast, $\dot{M}_{O_2}$ measured during swimming was not correlated with heart mass after accounting for body size (Odell et al., 2003). Similarly, Norin and Malte (2012) reported that mass-corrected ventricle size was unrelated to variation in MMR, SMR or AAS in brown trout. Together, these results suggest that the contribution of ventricle mass to variation in MMR in fishes may depend upon species or study design (e.g. among versus within population variation, see above).

Correlates of SMR

Traits related to the O_2 transport cascade that may limit maximum $\dot{M}_{O_2}$ are expected to exceed the much lower oxygen requirements at rest (Weibel et al., 1991) and, therefore, they may be poorly correlated or uncorrelated with SMR. Nevertheless, we found individual variation in SMR by *F. grandis* was positively correlated with TFL and with maximum uncoupled electron transport system respiration by myocardial mitochondria (ETS_{NS}) (Table 3). Notably, these relationships were both weaker for SMR than for MMR (Table 3) and accounted for 21% and 7%, respectively, of the mass-independent variation in SMR (Fig. 2). Three models were approximately equal in explaining variation in SMR (Table S2), and all included TFL as an important explanatory variable. Thus, we can reject the null hypothesis of no correlation between TFL and SMR. An association between TFL and SMR might have a mechanistic

basis. For example, larger gills represent a greater surface area for passive ion and water flux, which in turn requires active mechanisms to offset, thereby potentially elevating SMR (Gonzalez and Mcdonald, 1992). Alternatively, TFL could be mechanistically linked with MMR (see above) and also correlated with SMR because MMR and SMR are strongly, positively related in this species (Reemeyer and Rees, 2020). Further experiments are needed to distinguish between these possibilities; for example, assessing correlations between SMR and gill morphology or metabolism (Dawson et al., 2020) at various salinities.

Regarding the correlation between SMR of *F. grandis* and myocardial ETS_{NS}, the final model describing variation in SMR was only marginally more likely than a model that excluded ETS_{NS} (Table S2). Hence, the evidence supporting a correlation between myocardial metabolism and SMR by *F. grandis* is weak. Nevertheless, two recent studies in the closely related *F. heteroclitus* support a positive association between the $\dot{M}_{O_2}$ of whole hearts and RMR or SMR. Jayasundara et al. (2015) found that RMR measured at 28°C was significantly correlated (Spearman's rank=0.40) with 'basal' $\dot{M}_{O_2}$ of whole hearts (the average of three lowest rates with pyruvate as a substrate). Drown et al. (2021) investigated the relationships between SMR of *F. heteroclitus* acclimated to 12°C or 28°C with cardiac $\dot{M}_{O_2}$ in the presence of various metabolic substrates. After correcting for multiple comparisons, SMR at 12°C was positively correlated with cardiac $\dot{M}_{O_2}$ in the presence of lactate, ketones and ethanol, whereas SMR at 28°C was positively correlated with cardiac $\dot{M}_{O_2}$ fueled by endogenous substrates (no added substrates). However, because both studies used intact hearts, it is uncertain whether these relationships are due to individual variation in mitochondrial metabolism, substrate transport across the plasma membrane, or the amount of stored metabolic fuels.

Finally, our data allowed us to evaluate whether LEAK respiration was correlated with either SMR or MMR of *F. grandis*. Rolfe and Brown (1997) estimated that LEAK respiration by liver and skeletal muscle could account for up to 20–25% of BMR in mammals. In brown trout, Salin et al. (2016) found that interindividual variation in SMR correlated with LEAK respiration by liver mitochondria and variation in MMR correlated with LEAK respiration by skeletal muscle mitochondria. In addition, Mortensen and Gesser (1999) suggested that a significant portion of the $\dot{M}_{O_2}$ of rainbow trout cardiomyocytes at rest is due to LEAK. However, LEAK respiration is measured in the absence of ATP synthesis when the protonmotive force (Δp) is high. During ATP synthesis, the magnitude of Δp decreases across a range where LEAK respiration declines sharply (Nobes et al., 1990). Hence, the contribution of LEAK respiration to myocardial respiration *in vivo*, when the heart continuously synthesizes ATP at high rates, is likely to be minimal. Combined with the fact that the heart represents a small fraction of total body mass (Table 1), a quantitative relationship between the low rates of myocardial LEAK respiration (Fig. 1, Table 2) and whole-animal $\dot{M}_{O_2}$ seems unlikely. In the current study, myocardial LEAK respiration with either complex I substrates or complex I and II substrates was not found to be a significant predictor of either SMR or MMR. Hence, our results do not support an association between myocardial LEAK respiration and interindividual variation in whole-animal $\dot{M}_{O_2}$ by *F. grandis*.

Caveats and conclusions

As with any study that correlates *in vitro* results to *in vivo* performance, our interpretations come with caveats. First, the rates reported here should be considered maximum respiratory capacities because respiratory substrates, including oxygen, were maintained at saturating concentrations. Nevertheless, the values we report for myocardial $\dot{M}_{O_2}$ and the calculated cardiac power generation are comparable to values determined for intact, working fish hearts (Farrell and Smith, 2017; Rodnick and Gesser, 2017). Second, it is possible that differences in mitochondrial oxygen affinity (Cardinale et al., 2019; Chung et al., 2017; Larsen et al., 2011, 2020; Lau et al., 2017), ATP synthesis per mole of oxygen consumed (Salin et al., 2015, 2019) or respiratory substrates (Drown et al., 2021; Oleksiak et al., 2005) also contribute to interindividual variation in tissue and whole-animal $\dot{M}_{O_2}$. Third, this study focused on gill morphology and myocardial bioenergetics, which together explain 43% and 28% of the mass-independent variation in MMR and SMR, respectively. Metabolic rates are complex, polygenic traits (Bouchard et al., 1998; Hoppeler, 2018; Pettersen et al., 2018), and variables other than those measured here certainly contribute to variation among individuals.

Despite these caveats, however, this study is significant for several reasons. By demonstrating that variation in whole-animal $\dot{M}_{O_2}$ correlates with gill morphology and myocardial bioenergetics, the results support the idea that variation in aerobic metabolic rate is related to variation in subordinate traits comprising the O_2 transport cascade (Scott and Dalziel, 2021). Also, the results provide a link between myocardial bioenergetics and MMR, and by extension AAS, which represents the capacity for energetically expensive activities such as growth, foraging, digestion and locomotion (Claireaux and Lefrancois, 2007). Given that cardiac metabolism may be negatively impacted by anthropogenic climate alterations (Iftikar and Hickey, 2013) and contaminant releases (Kirby et al., 2019), the current results suggest that such impacts may extend to MMR, AAS and fitness-related activities. Furthermore, this study contributes to the growing appreciation of potential roles of mitochondria in animal energetics and ecology (Heine and Hood, 2020; Chung and Schulte, 2020; Koch et al., 2021; Sokolova, 2021). Finally, there are likely to be genetic bases for both gill morphology (Chapman et al., 2008) and myocardial bioenergetics (Baris et al., 2017); hence, variation in these traits among individuals within a population may respond to natural selection and influence the evolution of aerobic metabolism.

Acknowledgements

We thank T. E. Murphy, B. H. Price and J. Stampley for technical assistance and S. C. Hand for thoughtful discussions and critically reviewing the manuscript.

Competing interests

The authors declare no competing or financial interests.

Author contributions

Conceptualization: B.B.R., J.E.R., B.A.I.; Methodology: B.B.R., J.E.R.; Validation: B.B.R.; Formal analysis: B.B.R.; Investigation: B.B.R., J.E.R., B.A.I.; Resources: B.B.R., B.A.I.; Data curation: B.B.R.; Writing - original draft: B.B.R.; Writing - review & editing: B.B.R., J.E.R., B.A.I.; Visualization: B.B.R.; Supervision: B.B.R.; Project administration: B.B.R.; Funding acquisition: B.B.R., B.A.I.

Funding

Funding was provided by the Greater New Orleans Foundation.

Data availability

Data collected during this study are available from the Dryad digital repository (Rees et al., 2022): doi:10.5061/dryad.jsxksn0bx.

References

Baris, T. Z., Crawford, D. L. and Oleksiak, M. F. (2016). Acclimation and acute temperature effects on population differences in oxidative phosphorylation. *Am. J. Physiol. Regul. Integr. Comp. Physiol.* **310**, R185-R196. doi:10.1152/ajpregu.00421.2015

Baris, T. Z., Wagner, D. N., Dayan, D. I., Du, X., Blier, P. U., Pichaud, N., Oleksiak, M. F. and Crawford, D. L. (2017). Evolved genetic and phenotypic

differences due to mitochondrial-nuclear interactions. *PLoS Genet.* **13**, e1006517. doi:10.1371/journal.pgen.1006517

Bassett, D. R. and Howley, E. T. (2000). Limiting factors for maximum oxygen uptake and determinants of endurance performance. *Med. Sci. Sports Exerc.* **32**, 70-84. doi:10.1097/00005768-200001000-00012

Bouchard, C., Daw, E. W., Rice, T., Perusse, L., Gagnon, J., Province, M. A., Leon, A. S., Rao, D. C., Skinner, J. S. and Wilmore, J. H. (1998). Familial resemblance for VO2max in the sedentary state: the HERITAGE Family Study. *Med. Sci. Sports Exerc.* **30**, 252-258. doi:10.1097/00005768-199802000-00013

Brown, J. H., Gillooly, J. F., Allen, A. P., Savage, V. M. and West, G. B. (2004). Toward a metabolic theory of ecology. *Ecology* **85**, 1771-1789. doi:10.1890/03-9000

Burnham, K. P. and Anderson, D. J. (2002). *Model Selection and Multimodal Inference: a Practical Information-Theoretic Approach*. New York: Spring-Verlag.

Burton, T., Killen, S. S., Armstrong, J. D. and Metcalfe, N. B. (2011). What causes intraspecific variation in resting metabolic rate and what are its ecological consequences? *Proc. R. Soc. B Biol. Sci.* **278**, 3465-3473. doi:10.1098/rspb.2011.1778

Cardinale, D. A., Larsen, F. J., Jensen-Urstad, M., Rullman, E., Sondergaard, H., Morales-Alamo, D., Ekblom, B., Calbet, J. A. L. and Boushel, R. (2019). Muscle mass and inspired oxygen influence oxygen extraction at maximal exercise: role of mitochondrial oxygen affinity. *Acta Physiol.* **225**, e13110. doi:10.1111/apha.13110

Careau, V. and Garland, T., Jr (2012). Performance, personality, and energetics: correlation, causation, and mechanism. *Physiol. Biochem. Zool.* **85**, 543-571. doi:10.1086/666970

Chabot, D., Steffensen, J. F. and Farrell, A. P. (2016). The determination of standard metabolic rate in fishes. *J. Fish Biol.* **88**, 81-121. doi:10.1111/jfb.12845

Chapman, L. J., Chapman, C. A., Nordlie, F. G. and Rosenberger, A. E. (2002). Physiological refugia: swamps, hypoxia tolerance and maintenance of fish diversity in the Lake Victoria region. *Comp. Biochem. Physiol. A Mol. Integr. Physiol.* **133**, 421-437. doi:10.1016/S1095-6433(02)00195-2

Chapman, L. J., Albert, J. and Galis, F. (2008). Developmental plasticity, genetic differentiation, and hypoxia-induced trade-offs in an African cichlid fish. *Open Evol. J.* **2**, 75-88. doi:10.2174/1874404400802010075

Chung, D. J. and Schulte, P. M. (2020). Mitochondria and the thermal limits of ectotherms. *J. Exp. Biol.* **223**, jeb227801. doi:10.1242/jeb.227801

Chung, D. J., Morrison, P. R., Bryant, H. J., Jung, E., Brauner, C. J. and Schulte, P. M. (2017). Intraspecific variation and plasticity in mitochondrial oxygen binding affinity as a response to environmental temperature. *Sci. Rep.* **7**, 16238. doi:10.1038/s41598-017-16598-6

Claireaux, G. and Lefrancois, C. (2007). Linking environmental variability and fish performance: integration through the concept of scope for activity. *Philos. Trans. R. Soc. B Biol. Sci.* **362**, 2031-2041. doi:10.1098/rstb.2007.2099

Claireaux, G., McKenzie, D. J., Genge, A. G., Chatelier, A., Aubin, J. and Farrell, A. P. (2005). Linking swimming performance, cardiac pumping ability and cardiac anatomy in rainbow trout. *J. Exp. Biol.* **208**, 1775-1784. doi:10.1242/jeb.01587

Crawford, D. L. and Oleksiak, M. F. (2007). The biological importance of measuring individual variation. *J. Exp. Biol.* **210**, 1613-1621. doi:10.1242/jeb.005454

Dalziel, A. C., Ou, M. and Schulte, P. M. (2012). Mechanisms underlying parallel reductions in aerobic capacity in non-migratory threespine stickleback (*Gasterosteus aculeatus*) populations. *J. Exp. Biol.* **215**, 746-759. doi:10.1242/jeb.065425

Dalziel, A. C., Martin, N., Laporte, M., Guderley, H. and Bernatchez, L. (2015). Adaptation and acclimation of aerobic exercise physiology in Lake Whitefish ecotypes (*Coregonus clupeaformis*). *Evolution* **69**, 2167-2186. doi:10.1111/evo.12727

Dawson, N. J., Millet, C., Selman, C. and Metcalfe, N. B. (2020). Measurement of mitochondrial respiration in permeabilized fish gills. *J. Exp. Biol.* **223**, jeb216762. doi:10.1242/jeb.216762

de Jager, S. and Dekkers, W. J. (1975). Relations between gill structure and activity in fish. *Neth. J. Zool.* **25**, 276-308. doi:10.1163/002829675X00290

Doerrier, C., Garcia-Souza, L. F., Krumschnabel, G., Wohlfarter, Y., Mészáros, A. T. and Gnaiger, E. (2018). High-resolution fluorespirometry and OXPHOS protocols for human cells, permeabilized fibers and small biopsies of muscle, and isolated mitochondria. In *Mitochondrial Bioenergetics. Methods in Molecular Biology*, Vol. 1782 (ed. C. Palmeira and A. Moreno), pp. 31-70. New York, NY: Humana Press.

Driedzic, W. R. and Gesser, H. (1994). Energy metabolism and contractility in ectothermic vertebrate hearts: hypoxia, acidosis, and low temperature. *Physiol. Rev.* **74**, 221-258. doi:10.1152/physrev.1994.74.1.221

Drown, M. K., DeLiberto, A. N., Ehrlich, M. A., Crawford, D. L. and Oleksiak, M. F. (2021). Interindividual plasticity in metabolic and thermal tolerance traits from populations subjected to recent anthropogenic heating. *R. Soc. Open Sci.* **8**, 210440. doi:10.1098/rsos.210440

Duncan, W. P. (2020). Interspecific differences in the metabolic rate, gill dimension and hematology of fish in an Amazonian floodplain lake. *Aquatic Sci. Technol.* **8**, 38. doi:10.5296/ast.v8i1.15981

Eliason, E. J., Clark, T. D., Hague, M. J., Hanson, L. M., Gallagher, Z. S., Jeffries, K. M., Gale, M. K., Patterson, D. A., Hinch, S. G. and Farrell, A. P. (2011). Differences in thermal tolerance among sockeye salmon populations. *Science* **332**, 109-112. doi:10.1126/science.1199158

Evans, D. H. (1980). Osmotic and ionic regulation by freshwater and marine fishes. In *Environmental Physiology of Fishes* (ed. M. A. Ali), pp. 93-122. New York: Plenum Press.

Farrell, A. P. and Smith, F. (2017). Cardiac form, function and physiology. In *Fish Physiology*, Vol. 36A, (ed. A. P. Farrell and C. J. Brauner), pp. 155-264. Cambridge, MA: Academic Press.

Gillooly, J. F., Gomez, J. P., Mavrodiev, E. V., Rong, Y. and McLamore, E. S. (2016). Body mass scaling of passive oxygen diffusion in endotherms and ectotherms. *Proc. Natl. Acad. Sci. USA* **113**, 5340-5345. doi:10.1073/pnas.1519617113

Glazier, D. S. (2005). Beyond the '3/4-power law': variation in the intra- and interspecific scaling of metabolic rate in animals. *Biol. Rev. Camb. Philos. Soc.* **80**, 611-662. doi:10.1017/S1464793105006834

Gonzalez, R. J. and Mcdonald, D. G. (1992). The relationship between oxygen consumption and ion loss in a freshwater fish. *J. Exp. Biol.* **163**, 317-332. doi:10.1242/jeb.163.1.317

Heine, K. B. and Hood, W. R. (2020). Mitochondrial behavior, morphology, and animal performance. *Biol. Rev. Camb. Philos. Soc.* **95**, 730-737. doi:10.1111/brv.12584

Hillman, S. S., Hancock, T. V. and Hedrick, M. S. (2013). A comparative meta-analysis of maximal aerobic metabolism of vertebrates: implications for respiratory and cardiovascular limits to gas exchange. *J. Comp. Physiol. B Biochem. Syst. Environ. Physiol.* **183**, 167-179. doi:10.1007/s00360-012-0688-1

Hoppeler, H. (2018). Deciphering VO2 max: limits of the genetic approach. *J. Exp. Biol.* **221**, jeb164327. doi:10.1242/jeb.164327

Hoppeler, H. and Weibel, E. R. (1998). Limits for oxygen and substrate transport in mammals. *J. Exp. Biol.* **201**, 1051-1064. doi:10.1242/jeb.201.8.1051

Hughes, G. M. (1966). The dimensions of fish gills in relation to their function. *J. Exp. Biol.* **45**, 177-195. doi:10.1242/jeb.45.1.177

Hughes, G. M. (1984). General anatomy of the gills. In *Fish Physiology*, Vol. 10A (ed. W. S. Hoar and D. J. Randall), pp. 1-72. Orlando, FL: Academic Press.

Iftikar, F. I. and Hickey, A. J. R. (2013). Do mitochondria limit hot fish hearts? Understanding the role of mitochondrial function with heat stress in *Notolabrus celidotus*. *PLoS ONE* **8**, e64120. doi:10.1371/journal.pone.0064120

Jacobs, R. A. and Lundby, C. (2013). Mitochondria express enhanced quality as well as quantity in association with aerobic fitness across recreationally active individuals up to elite athletes. *J. Appl. Physiol.* **114**, 344-350. doi:10.1152/japplphysiol.01081.2012

Jayasundara, N., Kozal, J. S., Arnold, M. C., Chan, S. S. L. and Di Giulio, R. T. (2015). High-throughput tissue bioenergetics analysis reveals identical metabolic allometric scaling for teleost hearts and whole organisms. *PLoS ONE* **10**, e0137710. doi:10.1371/journal.pone.0137710

Karakelides, H., Irving, B. A., Short, K. R., O'Brien, P. and Nair, K. S. (2010). Age, obesity, and sex effects on insulin sensitivity and skeletal muscle mitochondrial function. *Diabetes* **59**, 89-97. doi:10.2337/db09-0591

Killen, S. S., Glazier, D. S., Rezende, E. L., Clark, T. D., Atkinson, D., Willener, A. S. T. and Halsey, L. G. (2016). Ecological influences and morphological correlates of resting and maximal metabolic rates across teleost fish species. *Am. Nat.* **187**, 592-606. doi:10.1086/685893

Kirby, A. R., Cox, G. K., Nelson, D., Heuer, R. M., Stieglitz, J. D., Benetti, D. D., Grosell, M. and Crossley, D. A., II (2019). Acute crude oil exposure alters mitochondrial function and ADP affinity in cardiac muscle fibers of young adult mahi-mahi (*Coryphaena hippurus*). *Comp. Biochem. Physiol. C Toxicol. Pharmacol.* **218**, 88-95. doi:10.1016/j.cbpc.2019.01.004

Koch, R. E., Buchanan, K. L., Casagrande, S., Crino, O., Dowling, D. K., Hill, G. E., Hood, W. R., McKenzie, M., Mariette, M. M., Noble, D. W. A. et al. (2021). Integrating mitochondrial aerobic metabolism into ecology and evolution. *Trends Ecol. Evol.* **36**, 321-332. doi:10.1016/j.tree.2020.12.006

Konarzewski, M. Książek, A. (2013). Determinants of intra-specific variation in basal metabolic rate. *J. Comp. Physiol. B* **183**, 27-41. doi:10.1007/s00360-012-0698-z

Kuznetsov, A. V., Veksler, V., Gellerich, F. N., Saks, V., Margreiter, R. and Kunz, W. S. (2008). Analysis of mitochondrial function in situ in permeabilized muscle fibers, tissues and cells. *Nat. Protoc.* **3**, 965-976. doi:10.1038/nprot.2008.61

Laporte, M., Dalziel, A. C., Martin, N. and Bernatchez, L. (2016). Adaptation and acclimation of traits associated with swimming capacity in lake whitefish (*Coregonus clupeaformis*) ecotypes. *BMC Evol. Biol.* **16**, 160. doi:10.1186/s12862-016-0732-y

Larsen, F. J., Schiffer, T. A., Sahlin, K., Ekblom, B., Weitzberg, E. and Lundberg, J. O. (2011). Mitochondrial oxygen affinity predicts basal metabolic rate in humans. *FASEB J.* **25**, 2843-2852. doi:10.1096/fj.11-182139

Larsen, F. J., Schiffer, T. A., Zinner, C., Willis, S. J., Morales-Alamo, D., Calbet, J. A. L., Boushel, R. and Holmberg, H. C. (2020). Mitochondrial oxygen affinity increases after sprint interval training and is related to the improvement in peak oxygen uptake. *Acta Physiol.* **229**, e13463. doi:10.1111/apha.13463

Larter, K. F. and Rees, B. B. (2017). Influence of euthanasia method on blood and gill variables in normoxic and hypoxic Gulf killifish *Fundulus grandis*. *J. Fish Biol.* **90**, 2323-2343. doi:10.1111/jfb.13316

Lau, G. Y., Mandic, M. and Richards, J. G. (2017). Evolution of cytochrome c oxidase in hypoxia tolerant sculpins (Cottidae, Actinopterygii). *Mol. Biol. Evol.* **34**, 2153-2162. doi:10.1093/molbev/msx179
Mahalingam, S., McClelland, G. B. and Scott, G. R. (2017). Evolved changes in the intracellular distribution and physiology of muscle mitochondria in high-altitude native deer mice. *J. Physiol.* **595**, 4785-4801. doi:10.1113/JP274130
McBryan, T. L., Healy, T. M., Haakons, K. L. and Schulte, P. M. (2016). Warm acclimation improves hypoxia tolerance in *Fundulus heteroclitus*. *J. Exp. Biol.* **219**, 474-484. doi:10.1242/jeb.133413
McNab, B. K. (1997). On the utility of uniformity in the definition of basal rate of metabolism. *Physiol. Zool.* **70**, 718-720. doi:10.1086/515881
McNab, B. K. (2002). *The Physiological Ecology of Vertebrates: a View from Energetics*. Ithaca, NY: Cornell University Press.
Memme, J. M., Erlich, A. T., Hood, D. A. and Phukan, G. (2021). Exercise and mitochondrial health. *J. Physiol. Lond.* **599**, 803-817. doi:10.1113/JP278853
Mortensen, B. and Gesser, H. (1999). O_2 consumption and metabolic activities in resting cardiac myocytes from rainbow trout. *J. Exp. Zool.* **283**, 501-509. doi:10.1002/(SICI)1097-010X(19990501)283:6<501::AID-JEZ1>3.0.CO;2-E
Moyes, C. D. (1996). Cardiac metabolism in high performance fish. *Comp. Biochem. Physiol. A Mol. Integr. Physiol.* **113**, 69-75. doi:10.1016/0300-9629(95)02057-8
Moyes, C. D. and Hood, D. A. (2003). Origins and consequences of mitochondrial variation in vertebrate muscle. *Annu. Rev. Physiol.* **65**, 177-201. doi:10.1146/annurev.physiol.65.092101.142705
Nespolo, R. F. and Franco, M. (2007). Whole-animal metabolic rate is a repeatable trait: a meta-analysis. *J. Exp. Biol.* **210**, 3877-3878. doi:10.1242/jeb.013110
Nobes, C. D., Brown, G. C., Olive, P. N. and Brand, M. D. (1990). Non-ohmic proton conductance of the mitochondrial inner membrane in hepatocytes. *J. Biol. Chem.* **265**, 12903-12909. doi:10.1016/S0021-9258(19)38245-6
Nordlie, F. G. (2006). Physicochemical environments and tolerances of cyprinodontoid fishes found in estuaries and salt marshes of eastern North America. *Rev. Fish Biol. Fish.* **16**, 51-106. doi:10.1007/s11160-006-9003-0
Norin, T. and Clark, T. D. (2016). Measurement and relevance of maximum metabolic rate in fishes. *J. Fish Biol.* **88**, 122-151. doi:10.1111/jfb.12796
Norin, T. and Malte, H. (2012). Intraspecific variation in aerobic metabolic rate of fish: relations with organ size and enzyme activity in brown trout. *Physiol. Biochem. Zool.* **85**, 645-656. doi:10.1086/665982
Odell, J. P., Chappell, M. A. and Dickson, K. A. (2003). Morphological and enzymatic correlates of aerobic and burst performance in different populations of Trinidadian guppies *Poecilia reticulata*. *J. Exp. Biol.* **206**, 3707-3718. doi:10.1242/jeb.00613
Oleksiak, M. F., Roach, J. L. and Crawford, D. L. (2005). Natural variation in cardiac metabolism and gene expression in *Fundulus heteroclitus*. *Nat. Genet.* **37**, 67-72. doi:10.1038/ng1483
Palzenberger, M. and Pohla, H. (1992). Gill surface area of water-breathing freshwater fish. *Rev. Fish Biol. Fish.* **2**, 187-216. doi:10.1007/BF00045037
Paradies, G., Paradies, V., De Benedictis, V., Ruggiero, F. M. and Petrosillo, G. (2014). Functional role of cardiolipin in mitochondrial bioenergetics. *Biochim. Biophys. Acta* **1837**, 408-417. doi:10.1016/j.bbabio.2013.10.006
Pesta, D. and Gnaiger, E. (2012). High-resolution respirometry: OXPHOS protocols for human cells and permeabilized fibers from small biopsies of human muscle. In *Mitochondrial Bioenergetics: Methods and Protocols, (Methods in Molecular Biology)*, Vol. 810 (ed. C. M. Palmeira and A. J. Moreno), pp. 25-58. Humana Press.
Pettersen, A. K., Marshall, D. J. and White, C. R. (2018). Understanding variation in metabolic rate. *J. Exp. Biol.* **221**, jeb166876. doi:10.1242/jeb.166876
Reemeyer, J. E. and Rees, B. B. (2020). Plasticity, repeatability, and phenotypic correlations of aerobic metabolic traits in a small estuarine fish. *J. Exp. Biol.* **223**, jeb228098. doi:10.1242/jeb.228098
Rees, B. B. and Matute, L. A. (2018). Repeatable interindividual variation in hypoxia tolerance in the Gulf killifish, *Fundulus grandis*. *Physiol. Biochem. Zool.* **91**, 1046-1056. doi:10.1086/699596
Rees, B., Reemeyer, J. and Irving, B. (2022). Data for Interindividual variation in maximum aerobic metabolism varies with gill morphology and myocardial bioenergetics in Gulf killifish. *Dryad, Dataset*. doi:10.5061/dryad.jsxksn0bx
Rezende, E. L., Garland, T., Jr, Chappell, M. A., Malisch, J. L. and Gomes, F. R. (2006). Maximum aerobic performance in lines of *Mus* selected for high wheel-running activity: effects of selection, oxygen availability and the mini-muscle phenotype. *J. Exp. Biol.* **209**, 115-127. doi:10.1242/jeb.01883
Rodnick, K. J. and Gesser, H. (2017). Cardiac energy metabolism. In *Fish Physiology*, Vol. 36A, (ed. A. P. Farrell and C. J. Brauner), pp. 317-367. Cambridge, MA: Academic Press.
Rolfe, D. F. S. and Brown, G. C. (1997). Cellular energy utilization and molecular origin of standard metabolic rate in mammals. *Physiol. Rev.* **77**, 731-758. doi:10.1152/physrev.1997.77.3.731
Salin, K., Auer, S. K., Rey, B., Selman, C. and Metcalfe, N. B. (2015). Variation in the link between oxygen consumption and ATP production, and its relevance for animal performance. *Proc. Biol. Sci.* **282**, 20151028. doi:10.1098/rspb.2015.1028
Salin, K., Auer, S. K., Rudolf, A. M., Anderson, G. J., Selman, C. and Metcalfe, N. B. (2016). Variation in metabolic rate among individuals is related to tissue-specific differences in mitochondrial leak respiration. *Physiol. Biochem. Zool.* **89**, 511-523. doi:10.1086/688769
Salin, K., Villasevil, E. M., Anderson, G. J., Lamarre, S. G., Melanson, C. A., McCarthy, I., Selman, C. and Metcalfe, N. B. (2019). Differences in mitochondrial efficiency explain individual variation in growth performance. *Proc. R. Soc. B* **286**, 20191466. doi:10.1098/rspb.2019.1466
Schmidt-Nielsen, K. (1997). *Animal Physiology*. Cambridge, UK: Cambridge University Press.
Scott, G. R. and Dalziel, A. C. (2021). Physiological insight into the evolution of complex phenotypes: aerobic performance and the O_2 transport pathway of vertebrates. *J. Exp. Biol.* **224**, jeb210849. doi:10.1242/jeb.210849
Sokolova, I. (2021). Bioenergetics in environmental adaptation and stress tolerance of aquatic ectotherms: linking physiology and ecology in a multi-stressor landscape. *J. Exp. Biol.* **224**, jeb236802. doi:10.1242/jeb.236802
Steinhausen, M. F., Sandblom, E., Eliason, E. J., Verhille, C. and Farrell, A. P. (2008). The effect of acute temperature increases on the cardiorespiratory performance of resting and swimming sockeye salmon (*Oncorhynchus nerka*). *J. Exp. Biol.* **211**, 3915-3926. doi:10.1242/jeb.019281
Svendsen, M. B. S., Bushnell, P. G. and Steffensen, J. F. (2016). Design and setup of intermittent-flow respirometry system for aquatic organisms. *J. Fish Biol.* **88**, 26-50. doi:10.1111/jfb.12797
Sylvestre, E.-L., Lapointe, D., Dutil, J.-D. and Guderley, H. (2007). Thermal sensitivity of metabolic rates and swimming performance in two latitudinally separated populations of cod, *Gadus morhua* L. *J. Comp. Physiol. B Biochem. Syst. Environ. Physiol.* **177**, 447-460. doi:10.1007/s00360-007-0143-x
Veksler, V. I., Kuznetsov, A. V., Sharov, V. G., Kapelko, V. I. and Saks, V. A. (1987). Mitochondrial respiratory parameters in cardiac tissue: a novel method of assessment by using saponin-skinned fibers. *Biochim. Biophys. Acta* **892**, 191-196. doi:10.1016/0005-2728(87)90174-5
Virani, N. A. and Rees, B. B. (2000). Oxygen consumption, blood lactate and inter-individual variation in the gulf killifish, *Fundulus grandis*, during hypoxia and recovery. *Comp. Biochem. Physiol. A Mol. Integr. Physiol.* **126**, 397-405. doi:10.1016/S1095-6433(00)00219-1
Wagner, P. D. (1996). Determinants of maximal oxygen transport and utilization. *Annu. Rev. Physiol.* **58**, 21-50. doi:10.1146/annurev.ph.58.030196.000321
Webber, D. M., Boutilier, R. G. and Kerr, S. R. (1998). Cardiac output as a predictor of metabolic rate in cod *Gadus morhua*. *J. Exp. Biol.* **201**, 2779-2789. doi:10.1242/jeb.201.19.2779
Weibel, E. R. and Hoppeler, H. (2005). Exercise-induced maximal metabolic rate scales with muscle aerobic capacity. *J. Exp. Biol.* **208**, 1635-1644. doi:10.1242/jeb.01548
Weibel, E. R., Taylor, C. R. and Hoppeler, H. (1991). The concept of symmorphosis: a testable hypothesis of structure-function relationship. *Proc. Natl. Acad. Sci. USA* **88**, 10357-10361. doi:10.1073/pnas.88.22.10357
Weibel, E. R., Bacigalupe, L. D., Schmitt, B. and Hoppeler, H. (2004). Allometric scaling of maximal metabolic rate in mammals: muscle aerobic capacity as determinant factor. *Respir. Physiol. Neurobiol.* **140**, 115-132. doi:10.1016/j.resp.2004.01.006
White, C. R. and Kearney, M. R. (2013). Determinants of inter-specific variation in basal metabolic rate. *J. Comp. Physiol. B* **183**, 1-26. doi:10.1007/s00360-012-0676-5
Zhang, Y., Gilbert, M. J. H. and Farrell, A. P. (2020). Measuring maximum oxygen uptake with an incremental swimming test and by chasing rainbow trout to exhaustion inside a respirometry chamber yields the same results. *J. Fish Biol.* **97**, 28-38. doi:10.1111/jfb.14311